


Review

Assessment of Soil Erosion Risk in Cultural Heritage Sites: A Bibliometric Analysis

Nikoletta Papageorgiou ^{1,*} , Diofantos Hadjimitsis ^{1,2}, Chris Danezis ^{1,2}  and Rosa Lasaponara ³

¹ Department of Civil Engineering and Geomatics, Faculty of Engineering and Technology, Cyprus University of Technology, Saripolou 2-8, 3036 Limassol, Cyprus; d.hadjimitsis@cut.ac.cy (D.H.); chris.danezis@cut.ac.cy (C.D.)

² Eratosthenes Centre of Excellence, 3012 Limassol, Cyprus

³ National Research Council—Institute of Methodologies for Environmental Analysis, C. da S. Loja, 85050 Tito Scalo, Italy; rosa.lasaponara@cnr.it

* Correspondence: nt.papageorgiou@edu.cut.ac.cy

Abstract

Different monitoring approaches and techniques have been adopted to estimate and prevent soil erosion and its corresponding phenomena at cultural heritage sites. Remote sensing plays a crucial role in detecting and monitoring soil erosion events by providing a wealth of geospatial data and information that helps to better understand and respond to the mechanisms of soil erosion and mitigate or reduce its impacts. The main aims of this review are to (1) provide an overview of remote sensing methods, applications, and sensor types, (2) discuss the role of remote sensing in the estimation of soil erosion at cultural heritage sites, and (3) present a bibliometric analysis of soil erosion studies at cultural heritage sites covering the period from 1994 to 2025. The results of this study provide insights into the yearly scientific production, methods employed, topics, and trends in this field. This research offers valuable information for future research and the development and promotion of policies and strategies for the effective and sustainable management of cultural heritage sites.

Keywords: cultural heritage; remote sensing; management; soil erosion; bibliometric analysis



Academic Editor: Károly Németh

Received: 28 May 2025

Revised: 26 July 2025

Accepted: 27 July 2025

Published: 30 July 2025

Citation: Papageorgiou, N.; Hadjimitsis, D.; Danezis, C.; Lasaponara, R. Assessment of Soil Erosion Risk in Cultural Heritage Sites: A Bibliometric Analysis. *Heritage* **2025**, *8*, 307. <https://doi.org/10.3390/heritage8080307>

Copyright: © 2025 by the authors. Licensee MDPI, Basel, Switzerland. This article is an open access article distributed under the terms and conditions of the Creative Commons Attribution (CC BY) license (<https://creativecommons.org/licenses/by/4.0/>).

1. Introduction

In recent times, soil erosion has become one of the most serious and escalating hydro-geological hazards [1] and is increasingly recognized as a key driver of the degradation of cultural heritage sites. Ongoing global climate change significantly influences soil erosion processes by modifying rainfall patterns, longer dry periods, increasing temperatures and atmospheric CO₂ concentrations, and reducing vegetation productivity and soil infiltration capacity [2–4]. Concurrently, soil erosion is further exacerbated by anthropogenic activities, including the cultivation, overgrazing, shifts in land use patterns and urban development which have led to an increased surface runoff, ultimately resulting in land deterioration [5–11].

Soil erosion is a slow and continual process that involves the detachment of soil material by rain as an erosive agent and its transportation through surface runoff and deposition [12,13]. It poses a multitude of environmental, economic, and social impacts, leading to the destruction of property, damage to infrastructure, and agricultural productivity decrease [14,15]. Notably, it is estimated that about 75 billion tons of soil worldwide

are degraded by soil erosion every year [16,17] costing approximately USD 400 billion in global financial losses [18], and it is projected to increase by 27–45% by 2090 [19]. Soil erosion has direct or indirect repercussions on the sustainability of archeological structures and stratigraphy. Direct impacts are the destruction of archeological contexts, altering the biochemical and physical mechanisms of historical building materials, and dispersing archeological artifacts on the surface [20]. Indirect impacts are materialized by secondary geomorphological hazards including desertification and landslides affecting the eroded areas, as well as from human responses to the erosion, including adaptive land use practices or construction activities.

Soil erosion processes and their potential impact on cultural heritage have been well documented in the existing literature [21–25]. However, relatively limited research has been conducted to identify and quantify the overall soil erosion risk and assess the vulnerability of heritage structures, intending to provide maximal protection, despite the widespread recognition that it is a growing critical issue. Given its significance, effective risk detection and prediction, vulnerability assessment, and decision-making are critical for monitoring the effects of soil erosion and for preserving and protecting these assets. In this context, international heritage authorities, including United Nations Educational, Scientific and Cultural Organization (UNESCO) and the International Council on Monuments and Sites (ICOMOS) have advocated for the incorporation of cultural heritage into disaster risk management strategies. For instance, the 2030 Agenda for Sustainable Development in 2015 emphasizes the necessity of risk estimation and damage assessment for cultural heritage. Specifically, Target 11.4, specifically calls for “Protect the world’s cultural and natural heritage-Strengthen efforts to protect and safeguard the world’s cultural and natural heritage” [26].

Soil erosion estimation of cultural heritage is a challenging task, partly due to the multi-faceted and heterogeneous nature of erosion processes, which are influenced by diverse environmental parameters with differing degrees of severity and spatial coverage. Historically, soil erosion management has been based on conventional methods, including plot experimental observations [27], direct field survey measurements [28–30], and visual inspection of aerial photographs and orthophotos. Although these methods can provide high precision in estimating soil erosion, they are expensive, labor-intensive, time-consuming, and not appropriate for calculating soil erosion risk in large areas [31].

To overcome these limitations, remote sensing is widely recognized as an indispensable non-destructive technological asset for the assessment of potential damage and identification of susceptible areas, allowing time series analysis in a relatively short time and at a low cost [32,33]. The emergence of various remote sensing platforms (satellites, UAVs, and airplanes) and sensors (active and passive) have become an alternative tool, providing data with higher spatial and temporal resolutions, operating on multiple wavelengths of the electromagnetic spectrum and various scales [34]. Simultaneously, with the increased availability of open access data, advances in space-borne sensors, and processing methods have substantially enriched the regular disaster management processes and decision-making. Remote sensing enables the quantification and determination of soil erosion risk factors and their mechanisms, analysis of spatio-temporal variations, predicting future scenarios and providing valuable information on climatic and topographical parameters, thus supporting future conservation management efforts [35–39].

To date, several review studies have been published in the field of soil erosion oriented towards the implementation of diverse remote sensing data sources, such as satellite imagery and UAV data. For example, Wang et al. [40] explore the use of remote sensing data sources and processing methods in soil erosion research. Ji et al. [41] summarized and assessed the effectiveness of satellite remote sensing methods for soil degradation

monitoring applications. Likewise, Medeiros et al. [42] conducted a systematic literature review of UAV applications in soil erosion monitoring, the recent advancements, integrated methods, and their limitations for soil erosion modeling. Meanwhile, Musasa et al. [43] presented a detailed overview of the use of Landsat data in soil degradation applications. Epple et al. [44] explored the performance of existing process-based soil erosion models in conjunction with remote sensing technologies. Sepuru and Dube [45] described soil erosion methods utilizing optical data for soil erosion monitoring. Although prior review papers pertain to the main topics and approaches of remotely sensed data for soil erosion research, there is no published comprehensive review specifically addressing the use of remote sensing applications for assessing and monitoring soil erosion processes and its potential impacts on cultural heritage sites.

To fill this gap, this review aims to provide an extensive bibliometric analysis of research progress and methodologies for soil erosion assessment and management, focusing on their practical applications in cultural heritage sites and their surrounding landscapes. The main objectives of this study were to (1) evaluate the role of remote sensing technologies in soil erosion assessment, while highlighting their advantages and drawbacks, and current challenges; (2) examine existing advanced methods used to estimate soil erosion in the reviewed literature, thereby contributing to a deeper understanding of ongoing advancements and identifying key trends and future research directions.

This paper is composed of five sections as follows: Section 2 provides a brief review of remote sensing platforms and sensors utilized in soil erosion research; Section 3 outlines the methodology employed in this review; Section 4 presents the main findings; Section 5 discusses the use of remote sensing technologies for estimating and modeling soil erosion at cultural heritage sites; and Section 6 delineates the final conclusions and recommendations for future work.

2. Remote Sensing Technologies for Soil Erosion Estimation

2.1. Optical Remote Sensing

Optical remote sensing, including very high resolution (VHR) and multispectral systems, captures information at several spectral bands ranging from visible to thermal infrared (TIR) spectral channels of the electromagnetic spectrum. Multispectral data are the most frequent source of information for soil erosion susceptibility mapping and assessment of vegetation changes [46]. Indeed, the availability of large open access data archives including those from the AVHRR (Advanced Very High Resolution Radiometer, 1.1 km) and MODIS (Moderate Resolution Imaging Spectroradiometer, 250–1000 m) aboard the TERRA and AQUA satellites, with low spatial resolutions and frequent revisit intervals were extensively used to identify periods of increased erosion risk, such as after heavy rainfall events or significant land use changes, particularly for large-scale applications. Long-term Landsat time series data collected by various spectral sensors, including the multispectral scanner (MSS) onboard Landsat 1–5, the Thematic Mapper (TM) onboard Landsat-4 and Landsat-5, the Enhanced Thematic Mapper (ETM+) on the Landsat 7 (1999) and the Operational Land Imager (OLI) on the Landsat 8 (2013) [47] have been utilized to detect and monitor soil erosion hazards across a range of scales [48]. Similarly, Copernicus Sentinel-2 constellation, consisting of two satellites, Sentinel-2A and Sentinel-2B, were launched in 2015 and 2017, respectively, which provide optical images with spatial resolution of 10 m to 60 m and a revisit time of five days, thereby facilitating detailed soil erosion mapping and detecting finer LULC changes. ASTER (Advanced Spaceborne Thermal Emission Reflection Radiometer) is a multispectral sensor that comprises 15 spectral bands mounted on NASA's Terra satellite, launched in 1999, with 15 m resolution (multispectral) and thermal infrared (TIR) with 30 m resolution and is suitable for assessing soil charac-

teristics, LULC monitoring [49–53], and enables the generation of Digital Elevation Model (DEM) or Digital Terrain Model (DTM) of the surveyed area [54].

Since 2000, very high resolution (VHR) commercial optical missions have been operated providing meter or submeter spatial resolution imagery that facilitates the development of more accurate disaster management applications [55,56]. For instance, the IKONOS sensor launched in 1999 has a spatial resolution of 4 m and 1 m panchromatic spatial resolution. The Quickbird satellite was launched in 2001 equipped with four-band (450–900 nm) and a 0.60 m resolution. Other commercial satellites include the Worldview satellites (2007–2009) that provide up to 1.8 m spatial resolution for the multispectral sensor and 1.1 days repeat cycle and GeoEye-1 deployed in 2008 with 0.50 m resolution (panchromatic) and 1.65 m (multispectral). Several studies explore the use of very high resolution (VHR) imagery using visual interpretation method to directly recognize the morphological (e.g., color, texture, shape) and lithological small scale features associated with erosion in satellite imagery based on expert knowledge [36]. Although these imageries are of very high quality, they are expensive, and therefore not easily applicable to large-scale and long-term monitoring studies. Moreover, optical imagery has inherent limitations under cloudy conditions, in shadowed areas, or during periods of low visibility, which can hinder consistent observation and analysis. Table 1 presents the most utilized optical satellites in soil erosion studies.

Table 1. Commonly used optical satellites sensors for soil erosion.

Sensor(s)	Launch Year	Spatial Resolution	Temporal Resolution	Spectral Range (µm)	Number of Bands
Landsat-1 MSS	1972	80	18	0.5–1.1	4
Landsat 2 MSS	1975	80	18	0.5–1.1	4
Landsat 3 MSS	1978	80	18	0.5–1.1	4
Landsat 4	1982	30	16	0.45–2.35	7
Landsat-5 TM	1984	30, 120	16	0.45–2.35	7
Landsat-7 ETM+	1999	15, 30, 60	16	0.45–12.5	8
Landsat 8 OLI	2013	15, 30	16	0.433–2.294	9
Sentinel-2 MSI	2015	10,20,60	5	0.443–2.202	13
AVHRR	1980	1100–5000	1	0.63–12	5
IKONOS	1999	4; 1	1.5–3	0.45–0.85	5
Quickbird	2001	0.6–2.6	2.4	450–900	5
ASTER	1999	15–90	16	0.52–2.43	15
MODIS	1999	250, 500, 1 km	1–2	0.459–2.155	36
Worldview 2	2009	0.5	1.1	450–800	9
Geoeye 1	2008	0.5–1.8	<3	450–920	5

2.2. Synthetic Aperture Radar (SAR)

Unlike optical sensors, SAR, as active microwave sensors, can operate day and night, independent of weather conditions and penetrating clouds or vegetation. SAR sensors operate at various microwave bands which are defined by their wavelengths, e.g., X-band with 3.1 cm, C-band with 5.6 cm, and L-band with 23.6 cm) [57,58], and have the capability to collect images over wide areas offering a high spatial resolution and frequent revisits. In this regard, the Sentinel-1 constellation is a C-band SAR system, composed of two satellites, Sentinel-1A and Sentinel-1B, with a temporal revisit interval of 6 to 12 days and down

to 5 m geometric resolution. Similarly, RADARSAT-2 launched in 2007 by the Canadian Space Agency (CSA), operates in the C-band microwaves (4~8 GHz) with a revisit time of 4 days [59]. TerraSAR-X mission led by the German Aerospace Center (DLR) in 2007, provides multimode X-band SAR data (8~12 GHz) in various modes (SpotLight (1 m), StripMap (3 m), and ScanSAR (40 m)-modes) [60]. COSMO-SkyMed X-band mission from the Italian Space Agency (ASI) provides high resolution radar images up to 1 m resolution, making them more suitable for detecting fine-scale erosion features [61]. SAR imagery has been used as an additional source of information to enhance the assessment and simulation of soil erosion patterns [37,61]. SAR data and Interferometric techniques, such as Differential Synthetic Aperture Radar Interferometry (DInSAR), InSAR Persistent Scatterer Synthetic Aperture Radar (PSInSAR), Short Baseline Subsets (SBAS), and Coherence Change Detection (CCD) are the most used methods. These techniques are utilized for detecting terrain and structural changes with millimeter accuracy by analyzing the phase difference (interferogram) between two SAR images acquired from the same orbit and location at different times [62]. Despite the advantages of using SAR data, according to a literature review, few scholars have explored SAR data for soil erosion applications [63–66]. The limited use of SAR is due to more complex interpretation of geometric distortions and speckle noise, making the change detection process more challenging compared to optical images [67].

2.3. Unmanned Aerial Vehicles (UAVs)

UAVs equipped with various sensors (e.g., red, green, and blue (RGB), thermal, multi-spectral, and hyperspectral cameras) present a useful tool for disaster damage assessment in complex or inaccessible landscapes [68]. These sensors collect high spatial resolution (submeter level) images [69], enabling the development of DEMs and ortho-image mosaics using numerous methods, such as the structure from motion (SfM) algorithm [70], DEMs of Difference (DoDs) [71], and Object-Based Image Analysis (OBIA). Even though UAVs have certain advantages, including low cost, easy-to-use, short revisit cycle, which make it a practical solution for small scale areas, they also present limitations, involving limited coverage area, climatic conditions restriction, and short battery life.

2.4. Remote Sensing Products

Satellite-derived products from various sources and platforms have become increasingly available to feed into soil erosion models, calibrate model variables, and validate simulated erosion processes (Table 2). The development of different types of remote sensing products at various spatial and temporal resolutions, such as LULC, meteorological, and topographic data, has facilitated the assessment and mapping of soil erosion hazards over time. Many studies have focused on using these products in soil erosion simulation and forecasting, either independently or in conjunction with other types of data.

Topographical information such as elevation, slope, and slope length has been the key input parameters for soil erosion models [72], which affect soil erosion rates and sediment deposition [73,74]. Traditionally, these morphological characteristics were manually derived from topographic maps, which provided a relatively low spatial resolution [75]. Recently, a variety of DEMs have been produced from optical satellite data [76], UAV photogrammetry data, and SAR interferometry [77,78]. The accuracy of these morphological characteristics is dependent on the source and resolution of the DEM used [79,80]. SAR and UAV technologies can generate terrain data with a meter-level resolution [81]. The most widely utilized global DEMs for soil erosion studies are the Shuttle Radar Topography Mission (SRTM, 30–90 m resolution) and the Advanced Spaceborne Thermal Emission and Reflection Radiometer (ASTER, 30 m resolution). Open access DEMs with coarse spatial

resolution, including Global Multi-resolution Terrain Elevation Data 2010 (GMTED 2010, 1000 m) and Global 30 Arc-Second Elevation (GTOPO-30, 1000 m) were used mainly in large-scale soil erosion modeling [82,83]. Precipitation significantly influences soil erosion formation and development [13].

Table 2. Characteristics of the most common satellite products used for soil mapping.

Indicator	Product	Spatial Resolution	Temporal Resolution	Data Availability
Rainfall	Tropical Rainfall Measuring Mission (TRMM)	0.25° × 0.25°	3 h	1997–2015
	Climate Hazards group Infrared Precipitation (CHIRP) V2.0	0.05° × 0.05°	Daily/5-day/10-day/monthly	1981–present
	Precipitation Estimation from Remotely Sensed Information using Artificial Neural Networks Cloud Classification System (PERSIANN-CCS)	0.04° × 0.04°	30 min	2003–present
	Precipitation Estimation from Remotely Sensed Information using Artificial Neural Networks (PERSIANN)	0.07° × 0.07°	6 h	1983–2016
	Climate Data Record (CDR) V1R1			
	Remotely Sensed Information using Artificial Neural Networks (PERSIANN)	0.04° × 0.04°	1 h	2000–present
	Global Precipitation Measurement (GPM)	0.1° × 0.1°	0.5–3 h	2014–present
Topography	Space Shuttle Radar Topography Mission (SRTM)	30–90 m	11 days	2000–present
	Advanced Spaceborne Thermal Emission and Reflection Radiometer Global Digital Elevation Model (ASTER GDEM)	30 m	-	2000–present
	Global Multi-resolution Terrain Elevation Data 2010 (GMTED 2010)	30 m	-	2010–present
	Global 30-Arc-Second Elevation Data Set (GTOPO30)	1 km	-	1996–present
Vegetation Cover	MODIS MOD12Q1	500 m	16 days	2001–2018
	MODIS MOD12Q1	1 km	16 days	2001–2018
	GlobLand30	30 m	-	2000–2010
	Esri’s 2020 Land Cover (Esri)	10 m	-	2020–present
	Google’s Dynamic World (DW)			2020–present
	ESA’s World Cover 2020 (WC)	10 m	-	2021–present
	Global Land Cover 2000 dataset	100 m	-	2000–present
	CLC1990	≤50 m	-	1986–1998
	CLC2000	≤25 m	-	2000 +/- 1 year
	CLC2006	≤25 m	-	2006 +/- 1 year
CLC2012	≤25 m	-	2012 +/- 1 year	
CLC2018	≤10 m (Sentinel-2)	-	2018 +/- 1 year	

Precipitation data are the main input in soil erosion models, as their high resolution and real-time data are essential for effective soil erosion assessment. Precipitation measurements are obtained by conventional methods such as rain gauge stations or satellite

observations. Rain gauge stations offer highly accurate point-based precipitation measurements, but their accuracy depends on their spatial distribution [84,85]. To address this limitation, various satellite precipitation products produced from passive microwave and infrared sensors have been developed as an alternative approach, offering broader spatial coverage and temporally continuous near real-time records on precipitation intensity, quantity, and erosivity [86]. Several scholars have examined the precision and reliability of satellite-based precipitation products, such as Climate Hazards Group Infrared Precipitation with Stations (CHIRPS), Tropical Rainfall Measuring Mission (TRMM) [87], Precipitation Estimation from Remotely Sensed Information Using Artificial Neural Networks (PERSIANN) [88], Precipitation Estimation from Remotely Sensed Information using Artificial Neural Networks–Cloud Classification System (PERSIANN-CCS), Precipitation Estimation from Remotely Sensed Information using Artificial Neural Networks–Climate Data Record (PERSIANN-CDR) [89], and the Global Precipitation Measurement (GPM) dataset [90] for soil erosion modeling [91–96]. Despite these advancements, these products are frequently subjected to considerable uncertainties and random errors due to sensor limitations, spatial resolution, and atmospheric interference. Consequently, some scholars have recommended the application of both satellite-based precipitation datasets and rain gauge measurements with various interpolation methods to enhance the accuracy of rainfall estimates [97–99].

Land cover plays a crucial role in regulating the intensity and frequency of soil erosion processes and land deterioration [100]. Changes in land use practices such as the transformation of natural lands (grasslands and forests) into urbanized areas and inadequate land management practices reduce vegetated areas and expose soil surfaces to precipitation, thereby increasing soil erosion susceptibility and sediment yield [3,101,102]. Hence, understanding the impact of land use/land cover (LULC) changes on soil erosion risk is of great significance for effective land use planning, environmental monitoring, and disaster prevention. Several studies have attempted to classify and map different land cover types using readily national or global LULC products based on different remotely sensed data at various spatial scales [103–111]. These products have frequently been utilized as inputs to estimate vegetative cover management (C-factor) based on table values from the sourced existing literature [112]. Typical products include the Coordination of Information on the Environment (CORINE) land cover map (CLC2000, CLC2006, CLC2012 and CLC2018) from the European Environmental Agency (EEA), GLOBELAND30 with 30 m spatial resolution produced by the National Geomatics Center of China [113], MODIS Land Cover type products (MCD12Q1 and MOD12Q1, 500/1000 m) produced by NASA [114], and Global Land Cover Map (GlobCover, 300 m) provided by the ESA [115]. Recently, three global LULC datasets, such as near real-time Google’s Dynamic World (DW), ESA’s World Cover 2020 (WC) [116], and Esri’s 2020 Land Cover (Esri) [117] with 10 m resolution, have been established based on Sentinel imagery. Although these LULC datasets provide valuable insights, they contain varying levels of uncertainty, which may limit their applicability for specific research contexts [118]. Thus, assessing the accuracy, consistency, and regional suitability of diverse LULC datasets is essential to ensure reliable analysis and informed decision-making.

3. Materials and Methods

3.1. Data Source Selection and Search Strategy

In this review, a systematic search of the published literature (scientific articles, reviews, conference papers, and book chapters) was conducted using the Scopus and Web of Science (WoS) databases platforms, last accessed on 17 July 2025, covering the period from 1994 to June 2025 (Table 3). The search was undertaken using the following query terms: “soil

erosion" AND "cultural heritage" OR "archaeological site" (query 1, Q1); "soil erosion" AND "cultural heritage" OR "archaeological site" AND "remote sensing" (query 2, Q2); "soil erosion" AND "cultural heritage" OR "archaeological site" AND "satellite imagery" (query 3, Q3); "soil erosion" AND "cultural heritage" OR "archaeological site" AND "SAR" OR "INSAR" (query 4, Q4); "soil erosion" AND "cultural heritage OR archaeological site" AND "UAV" OR "Drone" (query 5, Q5); "soil erosion" AND "cultural heritage" OR "archaeological site" AND "management" (query 6, Q6); "soil erosion" AND "cultural heritage" OR "archaeological site" AND "assessment" (query 7, Q7); and "soil erosion" AND "cultural heritage" OR "archaeological site" AND "modelling" (query 8, Q8).

Table 3. Statistics from the selected papers from Scopus and WoS platforms.

Description	Records	
	WoS	Scopus
Databases		
	67	118
	8	17
Query terms		
"soil erosion" AND "cultural heritage" OR "archaeological site" AND "satellite imagery"	3	5
"soil erosion" AND "cultural heritage" OR "archaeological site" AND "SAR" OR "INSAR"	1	4
"soil erosion" AND "cultural heritage OR archaeological site" AND "UAV" OR "Drone"	3	4
"soil erosion" AND "cultural heritage" OR "archaeological site" AND "management"	30	44
"soil erosion" AND "cultural heritage" OR "archaeological site" AND "assessment"	20	26
"soil erosion" AND "cultural heritage" OR "archaeological site" AND "modelling"	5	112
Time span	1998–June 2025	
Document type	Articles, book chapters, proceedings papers, reviews	
Language	English	

The eligibility criteria that were used throughout the search process were (1) papers published only in English and distributed in peer-reviewed journals and (2) studies directly related to soil erosion estimation, monitoring, and modeling, and excluded any other type of soil erosion research.

3.2. Data Screening, Analysis, and Visualization Strategy

A total of 137 and 230 peer-reviewed papers were retrieved and examined from the Web of Science and Scopus databases, respectively, based on the Preferred Reporting Items for Systematic Reviews and Meta-Analyses (PRISMA) method for the identification, screening, and eligibility of studies for inclusion in this review and meta-analysis, as illustrated in Figure 1. Subsequently, duplicate ($n = 36$) and non-English documents ($n = 10$) were removed, resulting in a total of 321 studies. Afterward, records were evaluated by subject fields that are closely related to soil erosion research in cultural heritage sites. As a result, 23 publications were discarded, as they were not relevant with the core themes of the review such as "Immunology and Microbiology" ($n = 1$), "Chemistry" ($n = 2$), "Plant sciences" ($n = 2$), "Geography Physical" ($n = 14$), "Biodiversity conservation" ($n = 2$), "Science and Ecology" ($n = 1$), "Energy" ($n = 5$), "Nuclear Science Technology" ($n = 1$), "Economics" ($n = 1$), and "Agricultural and Biological Sciences" ($n = 8$). The full texts of the remaining 298 articles were thoroughly examined to confirm their alignment with the research objectives. Finally, 54 articles that met all eligibility criteria were obtained and further analyzed in this bibliometric review using two open access bibliometric tools, namely the VOSviewer (version 1.6.20) and the Bibliometrix and Biblioshiny packages in Rstudio environment

(version: 2024.09.0-375). These tools facilitated the analysis of temporal research trends, collaborations network maps and keyword co-occurrences analysis related to research about soil erosion hazard over cultural heritage sites.

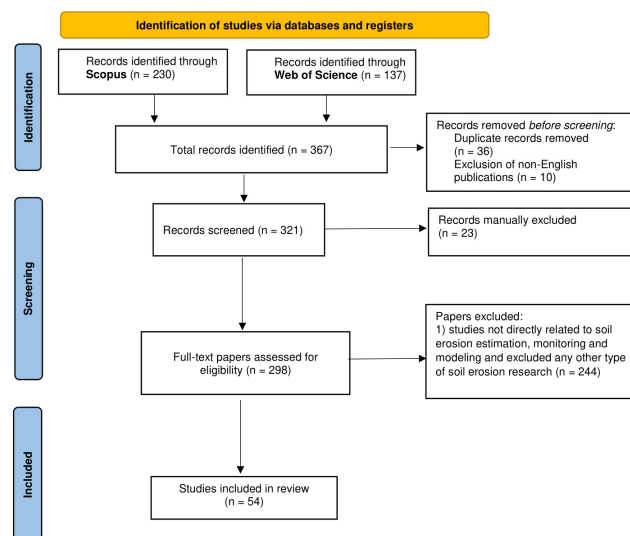


Figure 1. Overview of the research methodology.

4. Results

4.1. Spatial and Temporal Distribution of Published Studies

Figure 2 demonstrates the overall number of soil erosion-related documents affecting cultural heritage sites published each year from 1994 to June 2025. It can be observed that the number of publications was very low, with only a modest increase over the past decade, with the highest number of journals recorded in 2024. From 1994 to 2015, there were few academic studies in which the number of published articles was less than two per year. It indicates that the research on soil erosion was in its development phase, receiving limited scholarly attention during that period. Since 2016, the soil erosion topic has received considerable attention, showing relative stability in terms of the number of publications, corresponding to ~75.92% of the total number of publications. It is worth noting that no articles were identified in 1995–1997, 1999–2003, 2007, 2010 and 2012, indicating a potential absence of relevant research or a lack of available studies during those years.

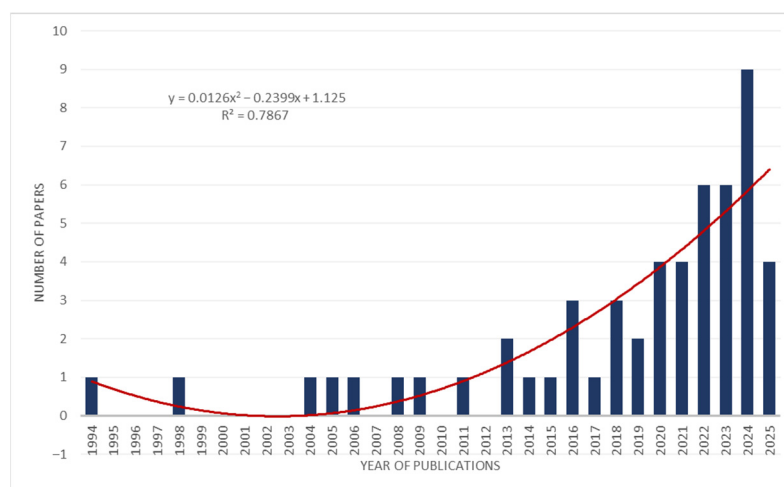


Figure 2. Number of papers relates to soil erosion studies in archeology (1994–2025) from Scopus and WoS platforms.

The 54 published papers included in this review were published in 38 scientific journals. Figure 3 depicts the first 10 sources with the most published articles. The Journal of Archeological Science had the most publications ($n = 5$), followed by Land ($n = 4$), International Journal of Disaster Risk Reduction ($n = 3$), and Remote Sensing ($n = 3$). The remaining six journals published only two articles each (for example, Geoarchaeology, Plos One, and Applied Geomatics), accounting for 13.95% of the total number of papers.

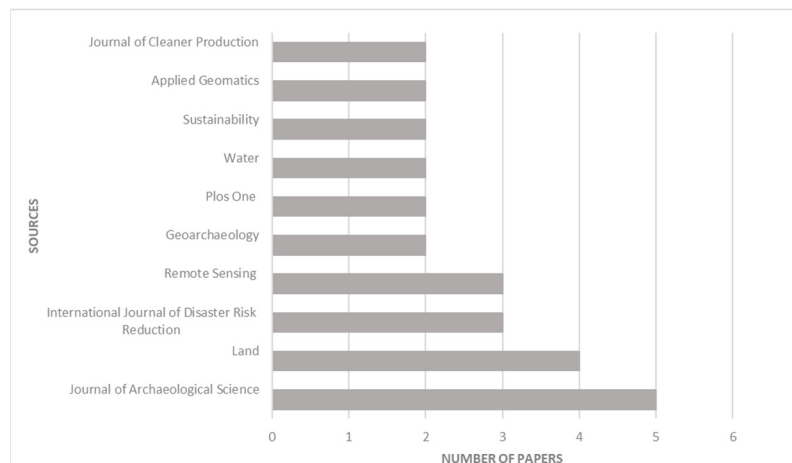


Figure 3. Journals of published articles.

The retrieved papers were classified into eight different thematic categories and disciplines according to the Scopus and WoS databases. As displayed in Figure 4, the highest proportion of these papers falls under Earth and Planetary Sciences (26%), followed by Social Sciences (23%) and Arts and Humanities (14%). Other frequently examined topics include Environmental Science (11%), Multidisciplinary (9%) and Computer Science (7%). Additionally, Material Science and Engineering account for the lower proportion at 5%, corresponding to three articles. It can be seen that individual articles may have been classified into multiple thematic categories, underscoring the high importance of environmental and geological and geomorphological issues, which are gaining growing attention within the scientific community.

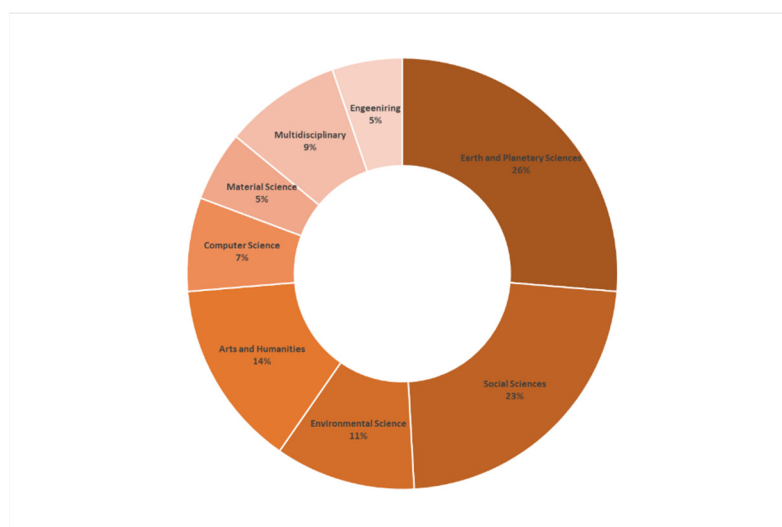


Figure 4. Thematic categories of published articles included in this review.

Figure 5 provides the geographic distribution of the top 10 countries involved in archeology and soil erosion research over the past three decades. As illustrated in Figure 5,

Italy has the highest number of publications ($n = 8$), reflecting the growing awareness of the scientific community of the potential soil erosion risk and its impacts on cultural heritage. This is followed by China, Greece, and Cyprus, which collectively account for 36.2% of all the analyzed publications. Other countries with notable contributions to this field include Romania ($n = 4$), the UK ($n = 3$), and Ethiopia, India, Jordan, and Germany, each with two relevant publications in this research topic.

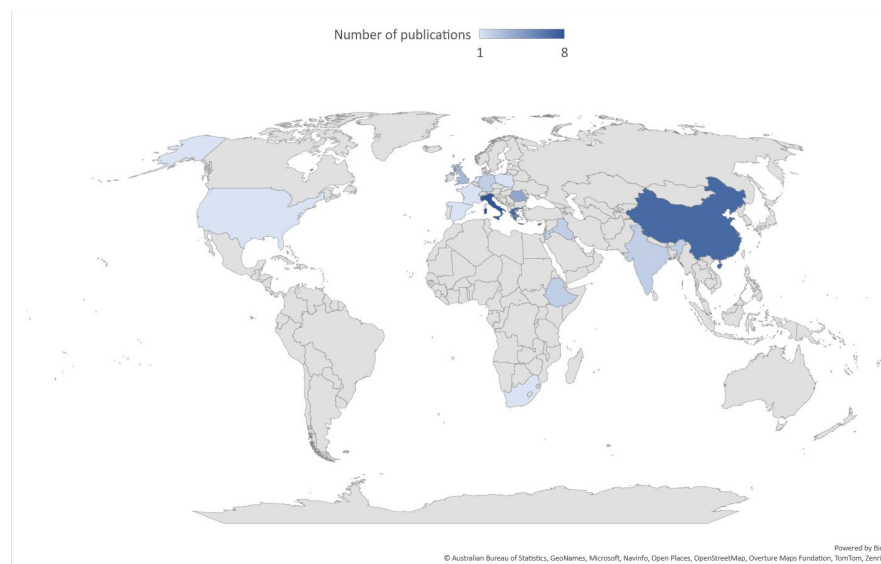


Figure 5. Spatial distribution of reviewed studies.

4.2. Co-Occurrence of Authors' Keywords

Figure 6a visualizes a co-occurrence network map of the most used authors' keywords based on the relevant research papers obtained from the Scopus and WoS search engines included in this study. As presented in Figure 6a, six clusters were identified. The first cluster (red color), the largest cluster, includes 10 keywords such as archeological sites, climate change, land use change, remote sensing, rusle, ndvi, and erosion. This cluster is centered on the potential of remote sensing technologies to estimate soil erosion processes under the impact of land use practices and climate change, involving published documents with topics dealing with various methods to analyze and interpret remote sensing data. The second cluster (green color) contains terms such as soil loss, soil erosion, usped model, and cultural heritage. This cluster emphasizes the importance of estimating and optimizing soil erosion processes in cultural heritage sites. Furthermore, the third cluster (blue color) encompasses keywords such as satellite remote sensing, landsat, rusle/usle, and risk assessment. This cluster reflects the strong link between technologies and soil erosion assessment, supporting the development of effective adaptation strategies and informed decision-making to mitigate adverse impacts on cultural heritage. The fourth cluster (yellow color) includes keywords such as management and natural hazards, which underscores the importance of integrated risk management and hazard assessment in erosion-prone areas. Lastly, the sixth cluster (light blue color) has 2 keywords associated with risk management and the application of GIS and remote sensing for mapping soil erosion rates and extent.

Figure 6b presents a density visualization map of the core keywords related to the topics of soil erosion in published papers. The terms "soil erosion", "cultural heritage", "climate change", "GIS", and "remote sensing" appear in high-density regions indicated by bright yellow, highlighting their relevance and the significant attention they have received from the academic community.

4.4. Thematic Map

The thematic map of author keywords related to soil erosion in archeological research from 1994 to 2025 is shown in Figure 8. The X-axis shows the centrality of a network cluster (degree of relevance), which assesses the importance of the theme within the research field, and the y-axis shows the density (degree of development). As can be seen from Figure 8, five clusters were produced in the thematic map of keywords. Cluster 1 and 2 located in the upper right quadrant (motor themes), indicates strong relevance and significant density encompassing terms such as remote sensing, climate change, and cultural heritage. Cluster 3, in the lower right quadrant (basic themes), has low centrality and high density. This cluster has limited importance in soil erosion studies. The cultural landscape theme appears twice in niche themes and in the basic themes. This cluster within the basic themes is significant for research, but further investigation is needed. Cluster 4, in the upper left quadrant (niche themes), includes keywords such as earth observation and satellite remote sensing have high density but limited importance to the core field. Cluster 4, in the lower left quadrant (emerging or declining themes), includes only one keyword (risk assessment), with low centrality and density.

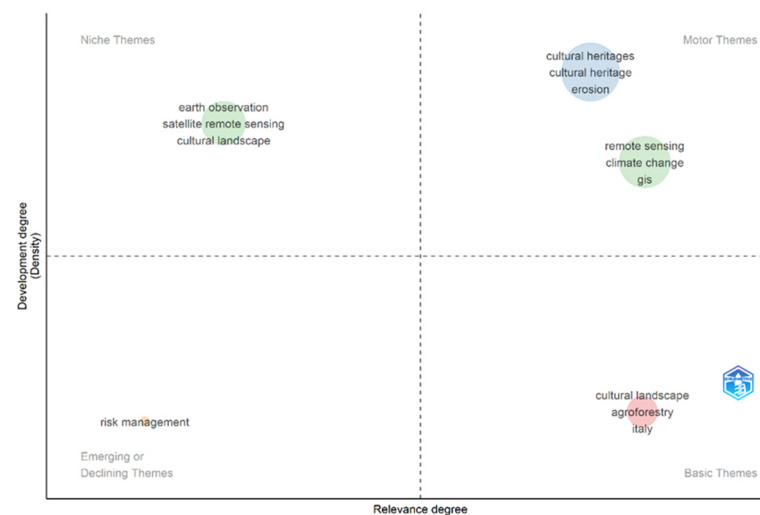


Figure 8. Thematic map of author keywords for 1994–2025 (R Studio Bibliometrix package).

5. Discussion

5.1. Methodologies

A number of qualitative and quantitative methods for estimating soil erosion on cultural heritage sites have been deployed in the examined research studies of the scientific literature. Each method has its own advantages and limitations, and the selection of an appropriate method depends on data availability, geographical and environmental characteristics of the study area, and specific research objectives.

Most of the studies used multidisciplinary approaches that integrated geomorphological methods, remote sensing techniques, and field surveys. Geomorphological approaches, including on-site surveys and laboratory analysis enable rapid, accurate, and repeatable measurements at the same site, they often rely on scale models and disturbed soil samples, which may limit their ability to accurately represent natural field conditions [119–121]. Furthermore, the collection of representative field data, especially under extreme rainfall events, necessitates long-term monitoring, which is a time-consuming and expensive process [122].

Alternatively, remote sensing technologies, including remote sensing imagery and UAV data, provide a valuable means for identifying soil erosion characteristics, model-

ing erosive factors across varying spatial and temporal scales and thus supporting the development of effective prevention and restoration strategies for safeguarding vulnerable heritage landscapes. The integration of diverse data sources and methods, such as soil erosion models, classification techniques, and band composite analysis and vegetation-related indices has significantly enhanced the interpretation of soil erosion processes while addressing spatial, temporal, and radiometric limitations. Among the various models applied to assess soil erosion risk, the Revised Universal Soil Loss Equation (RUSLE) [123] and the Unit Stream Power-based Erosion Deposition (USPED) model [124] are the most widely used for estimating long-term soil erosion rates and mapping high-risk zones due to moderate data requirements and simple structure. The RUSLE model calculates soil loss by considering various variables such as rainfall, topography and soil characteristics, while the USPED model estimates both erosion and deposition rates by considering sediment transport capacity.

Band composite analysis and vegetation-related indices based on the spectral reflectance of Visible (VIS—Blue/Green/Red) and Near Infrared (NIR) wavelengths from optical satellite images was also found to be one of the most commonly employed methods to assess vegetation condition, soil moisture, and assess crop type over time [125]. The most frequently used vegetation indices include the Normalized Difference Vegetation Index (NDVI). NDVI has been utilized as soil indicators or input data for the estimation of soil erosion models [126]. Higher NDVI values reflect dense vegetation that exhibit lower levels of soil erosion, as the vegetation acts as a protective barrier that shields the soil surface from the impact of raindrops and surface runoff [127].

Classification algorithms have also been employed for distinguishing eroded and non-eroded areas, identifying land use and soil cover, determining the extent of soil erosion on the surface, and evaluating spatial patterns through spectral characteristics to classify individual pixels into specific classes from remote sensing data. However, this approach has some limitations in detecting erosion features because (i) soil erosion varies spatially (size and shape), and temporally, and (ii) erosion-prone areas have similar spectral characteristics to other landscape features [128].

5.2. Applications Based on Remote Sensing for Soil Erosion Study in Cultural Heritage Sites

The potential of remote sensing technologies and their effectiveness have been explored in several cultural heritage sites in various countries such as Greece [129], Cyprus [130–134], Italy [135], UK [136], and Romania [137], demonstrating how these methods enable heritage monitoring across different scales.

Although the majority of studies implemented multispectral satellite data, such as Landsat and Sentinel-2, only a limited number have incorporated high resolution data, such as Quickbird [138] and Pleiades [139]. For example, Bagwan et Gavali [140] explored the capabilities of Landsat 8 and Sentinel-2 multispectral satellite imagery, rainfall, soil, and DEM data to study and quantify soil erosion risk using the RUSLE model in the UNESCO World Heritage site, Kaas Plateau, of India. The authors analyzed NDVI obtained from each satellite imagery at two different scales to evaluate vegetation variation. The authors concluded that appropriate spatial resolution of satellite data ensures accurate assessment of soil erosion factors. Polykretis et al. [141] studied the USPED empirical model to simulate the soil loss and deposition rates at various archeological sites over the Chania Prefecture of Crete (Greece). The proposed methodology includes freely available open access datasets such as Landsat-8 (OLI) imagery, rainfall data, elevation data gathered from the SRTM sensor, and land use/cover (LUCAS) observations. The results demonstrated that a considerable number of archeological sites situated in the west and north-east of the study area experienced high erosion rates. In their research, Guiney et al. [142] developed

a method for modeling soil erosion under future climate scenarios at the Roman fort of Magna, UK, using the CNRM-CM6-1 climate model, and the RUSLE model. For this purpose, various types of geospatial data such as Landsat imagery, aerial photography, and Lidar-derived DTM were used. The authors' findings emphasized the ability of the synergistic use of erosion models with rainfall erosivity values to identify areas that are susceptible to climate change in the future. Negula et al. [143] provided an example of the applicability of multi-temporal Sentinel-2, CORONA archive data, aerial photographs, and topographic maps to study the industrialization and soil erosion hazards at two archeological sites in Romania. The authors used three RS indices: NDVI, the Simple Ratio (SR) vegetation index, and the Normalized Difference Water Index (NDWI) to assess water content and crop parameters. The results showed that the synergistic use of remote sensing technologies can offer references for further studies to identify and monitor eroded cultural heritage areas. Pagels et al. [144] discussed the integrated use of the USPED model with a semi-automated classification algorithm based on TanDEM-X data to estimate erosion and deposition spatial patterns at the archeological site of Chintou, North Tunisia, aiming to determine geomorphological and sediment transport processes. Brandolini et al. [145] studied the impact of past land use practices on soil erosion rates in the Northern Apennines of Italy using the USPED model. The authors integrated various data, such as historical data, dendrochronology, and aerial and KH-9 (Hexagon) images to examine geomorphological changes under different scenarios linked to agroforestry systems. Their study revealed fluctuation in soil erosion rates, influenced by the distribution of agriculture over the study area. The same authors [146] applied the RUSLE model to demonstrate the impact of LULC changes on soil erosion in the Tuscan-Emilian Apennines (Italy). The authors illustrate how different historical farming practices can minimize soil erosion risk in response to current environmental conditions. In [147], used Landsat 5 TM and Sentinel-2 satellite images were integrated with the RUSLE model to produce soil erosion maps that examine the relationship between land use changes, as a result of urban expansion, and soil loss for the years 1987 and 2016 at the archeological site of Paphos area, Cyprus. The results of this paper revealed a clear correlation between land use transformations and increased soil erosion, highlighting the importance of monitoring such changes to protect archeological sites.

Additionally, several studies have used UAV-based remote sensing to produce high resolution DEM and orthophotos to capture more detailed surface characteristics, detect vegetation presence, and determine erosion features and sediment deposits. For instance, Wang et al. [148] employed UAV-acquired data and field sampling methods to estimate main driving factors of soil erosion under future climate scenarios along the Ming Great Wall in China. Likewise, Forti et al. [149] deployed high resolution UAV-based imagery integrated with the RUSLE model to examine soil and archeological sediments loss at two tell-sites in the Kurdistan Region of Iraq. The results, validated using field measurements, revealed spatial variability in soil loss rates influenced by morphometric characteristics. Ames et al. [150] assessed the impact of both past and future erosion risk on the spatial distribution of artifacts at open-air archeological sites in the Doring River (South Africa), using UAV-derived DTM and the RUSLE model. The authors proposed a prioritization framework for archeological research and conservation, recommending that sites facing a higher risk of erosion be prioritized for immediate investigation. Santos et al. [151] combined the RUSLE model along with CMIP6 climate models based on UAV-derived DEM and field data for measuring historical and future soil erosion risks at prehistoric sites in Ecuador.

5.3. Challenges and Opportunities

Soil erosion quantification and assessment present significant challenges due to the heterogeneous nature and behavior of the hazard and a range of uncertainties arising from the morphological representation of the cultural landscapes. As previously mentioned, soil erosion is a complex and ongoing process caused by several interactions and mechanisms, including precipitation conditions, vegetation coverage, and soil texture, which can occur at varying scales and variability over time. Effectively estimating the spatio-temporal dynamics of soil erosion and its driving mechanisms requires the integration of multidisciplinary approaches capable of extracting detailed insights about topographical, meteorological and geological and land use forces. Although remote sensing technologies offer substantial advantages in soil erosion research, they also present several challenges, particularly regarding spatial and temporal resolution of available datasets. The coarse spatial resolution limits their effectiveness in capturing detailed and accurate soil erosion estimation mainly to a local scale. Furthermore, assessing long-term changes in soil erosion is further restricted by the limited temporal resolution of available remote sensing datasets. While high spatial resolution optical sensors have demonstrated superior efficiency in assessing soil erosion, their application remains limited in comparison to multispectral data due to their high cost and lower resolution. UAVs have also faced significant limitations related to flight range, battery life, and data processing capacity.

The fusion of multi-sensor datasets offers potential for improving the precision of soil erosion assessment; however, it also entails additional challenges related to data harmonization, increased computational resource demands, and the need for advanced analytical algorithms. To overcome these challenges, the synergistic use of remote sensing, ground surveys, and ground truth data can greatly enhance more precise evaluations of soil erosion and influencing factors.

6. Conclusions

This review quantitatively examined and discussed processing methods and recent advances and procedures for soil erosion at cultural heritage sites, showcasing the overall trends, the input data, and output results from 1994 to 2025. Furthermore, it examined the limitations of existing studies and outlined future directions for soil erosion research. A bibliometric analysis of 54 published papers provided by the Scopus and WoS databases revealed that the study of soil erosion at cultural heritage has garnered minimal attention from the scientific community and local stakeholders. The main outcomes of the analysis can be summarized as follows:

- (1) From 1994 to 2014, the annual number of publications was small, with only one or no publications each year. Since 2016, there was a slight increase, showing relative stability in the number of publications. This trend may be attributed to significant advancements in remote sensing, data accessibility, and processing techniques.
- (2) The majority of articles focused on cultural heritage sites in the Mediterranean region, which are more susceptible to soil erosion hazards induced by extreme weather events due to complex topography and heterogeneous environment with steep slope areas accounting for 31.7% of the total publications.
- (3) Optical data, such as open access multi-temporal Landsat (TM, ETM+, and OLI) and Sentinel 2 A/B (MSI) are mainly implemented in the reviewed studies for soil erosion observations. UAV data is applied in a significant number of papers. Additionally, few studies employed more than one sensor for estimating soil erosion to improve spatial or temporal coverage continuity and overall accuracy.
- (4) A wide array of remote sensing-based approaches for quantitative assessment are suggested in the literature, such as soil erosion models and spectral indices. These

approaches combined with spatial datasets have been effectively employed for understanding soil erosion conditions and the regulatory mechanisms of soil erosion vulnerability. Notably, soil erosion models integrating with terrain, satellite, and precipitation data have become essential in remote sensing-based soil management research for calculating soil erosion rates and determining main triggering factors of soil degradation. Spectral indices such as NDVI were the primarily utilized indicator to study vegetation conditions.

Soil erosion estimation and management at cultural heritage sites exhibit significant regional variation, with the extent and distribution of erosion influenced by natural forces, climatic conditions, and human activities. Thus, monitoring of cultural heritage sites necessitates a multidisciplinary approach encompassing various perspectives, including geomorphological, topographical, and environmental information, leading to improved prevention strategies such as land use planning and vegetation restoration to control and minimize the severity of hazards.

The use of remote sensing technologies in the soil erosion field enables researchers to acquire information about soil erosion with greater precision and efficiency. Moreover, spatial and temporal limitations, accessibility, and high cost have constrained the widespread adoption of remote sensing data. Integrating remote sensing methods with field data supports a more comprehensive understanding of erosion processes.

In conclusion, this study provides insights into current trends, highlights existing gaps, and outlines future directions in soil erosion research particularly in the context of cultural heritage sites. It also emphasizes the importance of advancing monitoring techniques to improve protection and management strategies.

Despite its contribution, this study has several shortcomings. Firstly, this study used Scopus and WoS databases as the main data sources. Future research could incorporate additional bibliometric databases to enhance the collection and the analysis of a broader range of published articles could offer a more holistic view of the field. Secondly, further work is required to investigate the possibilities of in situ or ground-based platforms, optimize methodologies, and integrate data from various sources aimed at delivering more reliable and accurate results for effective soil erosion research to improve management practices.

Author Contributions: Conceptualization, N.P., D.H., C.D. and R.L.; methodology, N.P. and D.H.; software, N.P.; validation, N.P. and D.H.; formal analysis, N.P.; investigation, N.P.; resources, D.H.; data curation, N.P.; writing—original draft preparation, N.P.; writing—review and editing, N.P., D.H., C.D. and R.L.; visualization, N.P., D.H., C.D. and R.L.; supervision, D.H. All authors have read and agreed to the published version of the manuscript.

Funding: The APC was funded by Cyprus University of Technology.

Data Availability Statement: Data are contained within the article.

Acknowledgments: The authors would like to acknowledge the “CUT Open Access Author Fund” for covering the open access publication fees of the paper. The authors would like to thank the ERATOSTHENES Center of Excellence (ECoE) & ‘EXCELSIOR’ H2020 Widespread Teaming project (www.excelsior2020.eu). The ‘ERATOSTHENES: Excellence Research Centre for Earth Surveillance and Space-Based Monitoring of the Environment’- ‘EXCELSIOR’ project received funding from the European Union’s Horizon 2020 research and innovation program under Grant Agreement No. 857510 and from the Government of the Republic of Cyprus through the Directorate General for the European Programms, Coordination and Development.

Conflicts of Interest: The authors declare no conflicts of interest.

References

1. European Commission (EC). Proposal for a Directive of the European Parliament and of the Council Establishing a Framework for the Protection of Soil and Amending Directive 2004/35/ec (com (2006)232). 2006. Available online: <http://eur-lex.europa.eu/legal-content/EN/TXT/?uri=CELEX%3A52006PC0232> (accessed on 7 March 2025).
2. Li, Z.; Fang, H. Impacts of climate change on water erosion: A review. *Earth-Sci. Rev.* **2016**, *163*, 94–117. [CrossRef]
3. Borrelli, P.; Robinson, D.A.; Panagos, P.; Ballabio, C. Land use and climate change impacts on global soil erosion by water (2015–2070). *Proc. Natl. Acad. Sci. USA* **2020**, *117*, 21994–22001. [CrossRef]
4. Pimentel, D.; Harvey, C.; Resosudarmo, P.; Sinclair, K.; Kurz, D.; McNair, M.; Crist, S.; Sphpritz, L.; Fitton, L.; Saffouri, R.; et al. Environmental and economic costs of soil erosion and conservation benefits. *Science* **1995**, *267*, 1117–1123. [CrossRef]
5. Tamene, L.; Park, S.J.; Dikau, R.; Vlek, P.L.G. Analysis of factors determining sediment yield variability in the highlands of northern Ethiopia. *Geomorphology* **2006**, *76*, 76–91. [CrossRef]
6. Blanco, H.; Lal, R. *Principles of Soil Conservation and Management*; Springer: New York, NY, USA, 2008; pp. 167–169.
7. Ali, M.G.; Ali, S.; Arshad, R.H.; Nazeer, A.; Waqas, M.M.; Waseem, M.; Aslam, R.A.; Cheema, M.J.M.; Leta, M.K.; Shauket, I. Estimation of Potential Soil Erosion and Sediment Yield: A Case Study of the Transboundary Chenab River Catchment. *Water* **2021**, *13*, 3647. [CrossRef]
8. Islam, F.; Ahmad, M.N.; Janjuhah, H.T.; Ullah, M.; Islam, I.U.; Kontakiotis, G.; Skilodimou, H.D.; Bathrellos, G.D. Modelling and Mapping of Soil Erosion Susceptibility of Murree, Sub-Himalayas Using GIS and RS-Based Models. *Appl. Sci.* **2022**, *12*, 12211. [CrossRef]
9. Carollo, F.G.; Nicosia, A.; Palmeri, V.; Pampalona, V.; Serio, M.A.; Ferro, V. Measuring Rainfall Kinetic Power in Two Sicilian Experimental Areas by Drop-Size Distribution Data. *Land* **2023**, *12*, 418. [CrossRef]
10. Bryan, R.B.; Campell, J. Runoff and sediment discharge in a semiarid ephemeral drainage basin. *Z. Für Geomorphol. Suppl.* **1986**, *58*, 121–143.
11. Mitchell, D.J. The use of vegetation and land use parameters in modelling catchment sediment yields. In *Vegetation and Erosion: Processes and Environments*; Thomes, J.B., Ed.; Wiley: Chichester, UK, 1990; pp. 289–314.
12. Zachar, D. *Soil Erosion*; Cowan, M., Ed.; Elsevier Scientific Pub. Co.: New York, NY, USA, 1982. Available online: https://scholar.google.com/scholar?hl=en&as_sdt=0%2C5&q=12.%09Zachar%2C+D.+Soil+Erosion%3B+Cowan%2C+M.%2C+Ed.%3B+Elsevier+Scientific+Pub.+Co.%3A+New+York%2C+NY%2C+USA%2C+1982.&btnG= (accessed on 7 March 2025).
13. Kinnell, P.I.A. Raindrop impact—Induced erosion processes and prediction—A review. *Hydrol. Process* **2005**, *19*, 2815–2844. [CrossRef]
14. Nearing, M.A.; Pruski, F.F.; O’neal, M.R. Expected climate change impacts on soil erosion rates: A review. *J. Soil Water Conserv.* **2004**, *59*, 43–50. [CrossRef]
15. Morgan, R.P.C. *Soil Erosion and Conservation*, 3rd ed.; Blackwell Publishing Ltd.: Malden, MA, USA, 2005. [CrossRef]
16. Gong, W.; Liu, T.; Duan, X.; Sun, Y.; Zhang, Y.; Tong, X.; Qiu, Z. Estimating the Soil Erosion Response to Land-Use Land-Cover Change Using GIS-Based RUSLE and Remote Sensing: A Case Study of Miyun Reservoir, North China. *Water* **2022**, *14*, 742. [CrossRef]
17. Borrelli, P.; Robinson, D.A.; Fleischer, L.R.; Lugato, E.; Ballabio, C.; Alewell, C.; Meusburger, K.; Modugno, S.; Schütt, B.; Ferro, V.; et al. An assessment of the global impact of 21st century land use change on soil erosion. *Nat. Commun.* **2017**, *8*, 2013. [CrossRef] [PubMed]
18. Camacho-Zorogastúa, K.d.C.; Cesar Minga, J.; Gómez-Lora, J.W.; Gallo-Ramos, V.H.; Garcés Díaz, V. Evaluation of Soil Loss and Sediment Yield Based on GIS and Remote Sensing Techniques in a Complex Amazon Mountain Basin of Peru: Case Study Mayo River Basin, San Martin Region. *Sustainability* **2023**, *15*, 9059. [CrossRef]
19. Xiong, M.; Guoyong, L. Global soil water erosion responses to climate and land use changes. *Catena* **2024**, *241*, 108043. [CrossRef]
20. Agapiou, A.; Lysandrou, V.; Hadjimitsis, D.G. A European-Scale Investigation of Soil Erosion Threat to Subsurface Archaeological Remains. *Remote Sens.* **2020**, *12*, 675. [CrossRef]
21. Pederson, J.L.; Petersen, P.A.; Dierker, J.L. Gullying and erosion control at archaeological sites in Grand Canyon, Arizona. *Earth Surf. Proc. Landf.* **2006**, *31*, 507–525. [CrossRef]
22. Robinson, M.H.; Alexander, C.R.; Jackson, C.W.; McCabe, C.P.; Crass, D. Threatened archaeological, historic, and cultural resources of the Georgia Coast: Identification, prioritization and management using GIS technology. *Geoarchaeology* **2010**, *25*, 312–326. [CrossRef]
23. Meylemans, E.; Poesen, J.; In’t Ven, I. *The Archaeology of Erosion, the Erosion of Archaeology: Proceedings of the Brussels Conference, April 28–30, 2008*; Flanders Heritage Agency: Brussels, Belgium, 2017. [CrossRef]
24. Wilkinson, K.; Tyler, A.; Davidson, D.; Grieve, I. Quantifying the threat to archaeological sites from the erosion of cultivated soil. *Antiquity* **2006**, *80*, 658–670. [CrossRef]

25. Bell, M.; Boardman, J. *Past and Present Soil Erosion (Oxbow Monograph)*; Oxbow Books: Oxford, UK, 1992. Available online: https://scholar.google.com/scholar?hl=en&as_sdt=0%2C5&q=25.%09Bell%2C+M.%3B+Boardman%2C+J.+Past+and+Present+Soil+Erosion+%28Oxbow+Monograph%29%3B+Oxbow+Books%3A+Oxford%2C+UK%2C+1992.&btnG= (accessed on 7 March 2025).
26. UN. *Transforming Our World: The 2030 Agenda for Sustainable Development*; UN Doc. A/RES/70/1 (25 September 2015); UN: San Francisco, CA, USA, 2015. Available online: <https://undocs.org/en/A/RES/70/1> (accessed on 7 March 2025).
27. Porat, N.; López, G.I.; Lensky, N.; Elinson, R.; Avni, Y.; Elgart-Sharon, Y.; Faershtein, G.; Gadot, Y. Using portable OSL reader to obtain a time scale for soil accumulation and erosion in archaeological terraces, the Judean Highlands, Israel. *Quat. Geochronol.* **2019**, *49*, 65–70. [[CrossRef](#)]
28. Gonnet, A.; Todisco, D.; Rasse, M.; Mouralis, D.; Lepert, T. Soil erosion and anthropogenic impact on landscape evolution over the past 2500 years: A case study of the Villers-Ecalles dry valley (Seine-Maritime, Normandy, France). *Geomorphology* **2023**, *427*, 108623. [[CrossRef](#)]
29. Kappler, C.; Kaiser, K.; Tanski, P.; Klos, F.; Fülling, A.; Mrotzek, A.; Sommer, M.; Bens, O. Stratigraphy and age of colluvial deposits indicating Late Holocene soil erosion in northeastern Germany. *Catena* **2018**, *170*, 224–245. [[CrossRef](#)]
30. Leopold, M.; Völkel, J. Reconstruction of the old cultural surface of a Bronze Age Settlement—An example for a multi-methodological interaction of Soil Science and Archaeology in Southern Germany. *Geodin. Acta* **2007**, *20*, 257–265. [[CrossRef](#)]
31. Nicosia, A.; Carollo, F.G.; Di Stefano, C.; Palmeri, V.; Pampalone, V.; Serio, M.A.; Bagarello, V.; Ferro, V. The Importance of Measuring Soil Erosion by Water at the Field Scale: A Review. *Water* **2024**, *16*, 3427. [[CrossRef](#)]
32. Xu, S.; Wang, X.; Ma, X.; Gao, S. Risk Assessment and Prediction of Soil Water Erosion on the Middle Northern Slope of Tianshan Mountain. *Sustainability* **2023**, *15*, 4826. [[CrossRef](#)]
33. Valkanou, K.; Karymbalis, E.; Bathrellos, G.; Skilodimou, H.; Tsanakas, K.; Papanastassiou, D.; Gaki-Papanastassiou, K. Soil Loss Potential Assessment for Natural and Post-Fire Conditions in Evia Island, Greece. *Geosciences* **2022**, *12*, 367. [[CrossRef](#)]
34. Zingaro, M.; Scicchitano, G.; Capolongo, D. The Innovative Growth of Space Archaeology: A Brief Overview of Concepts and Approaches in Detection, Monitoring, and Promotion of the Archaeological Heritage. *Remote Sens.* **2023**, *15*, 3049. [[CrossRef](#)]
35. Vrieling, A. Satellite remote sensing for water erosion assessment: A review. *Catena* **2006**, *65*, 2–18. [[CrossRef](#)]
36. King, C.; Baghdadi, N.; Lecomte, V.; Cerdan, O. The application of remote-sensing data to monitoring and modelling of soil erosion. *Catena* **2005**, *2*, 79–93. [[CrossRef](#)]
37. Dwivedi, R.S.; Kumar, A.B.; Tewari, K.N. The utility of multisensory data for mapping eroded lands. *Int. J. Remote Sens.* **1997**, *18*, 2303–2318. [[CrossRef](#)]
38. Hall, F.G.; Townshend, J.R.; Engman, E.T. Status of remote-sensing algorithms for estimation of land-surface state parameters. *Remote Sens. Environ.* **1995**, *51*, 138–156. [[CrossRef](#)]
39. Joshi, N.; Baumann, M.; Ehammer, A.; Fensholt, R.; Grogan, K.; Hostert, P.; Jepsen, M.R.; Kuemmerle, T.; Meyfroidt, P.; Mitchard, E.T.A.; et al. A Review of the Application of Optical and Radar Remote Sensing Data Fusion to Land Use Mapping and Monitoring. *Remote Sens.* **2016**, *8*, 70. [[CrossRef](#)]
40. Wang, J.; Yang, J.; Li, Z.; Ke, L.; Li, Q.; Fan, J.; Wang, X. Research on Soil Erosion Based on Remote Sensing Technology: A Review. *Agriculture* **2025**, *15*, 18. [[CrossRef](#)]
41. Ji, C.; Cao, Y.; Li, X.; Pei, X.; Sun, B.; Yang, X.; Zhou, W. A review of the satellite remote sensing techniques for assessment of runoff and sediment in soil erosion. *J. Hydrol. Hydromech.* **2024**, *72*, 252–267. [[CrossRef](#)]
42. Medeiros, B.M.; Cândido, B.; Jimenez, P.A.J.; Avanzi, J.C.; Silva, M.L.N. UAV-Based Soil Water Erosion Monitoring: Current Status and Trends. *Drones* **2025**, *9*, 305. [[CrossRef](#)]
43. Musasa, T.; Dube, T.; Marambanyika, T. Landsat satellite programme potential for soil erosion assessment and monitoring in arid environments: A review of applications and challenges. *Int. Soil Water Conserv. Res.* **2023**, *12*, 267–278. [[CrossRef](#)]
44. Epple, L.; Kaiser, A.; Schindewolf, M.; Bienert, A.; Lenz, J.; Eltner, A. A Review on the Possibilities and Challenges of Today's Soil and Soil Surface Assessment Techniques in the Context of Process-Based Soil Erosion Models. *Remote Sens.* **2022**, *14*, 2468. [[CrossRef](#)]
45. Sepuru, T.K.; Dube, T. An appraisal on the progress of remote sensing applications in soil erosion mapping and monitoring. *Remote Sens. Appl. Soc. Environ.* **2018**, *9*, 1–9. [[CrossRef](#)]
46. Colwell, R.N. (Ed.) *Manual of Remote Sensing*, 2nd ed.; American Society for Photogrammetry and Remote Sensing: Falls Church, Virginia, 1983.
47. Wulder, M.A.; White, J.C.; Loveland, T.R.; Woodcock, C.E.; Belward, A.S.; Cohen, W.B.; Fosnight, E.A.; Shaw, J.; Masek, J.G.; Roy, D.P. The global Landsat archive: Status, consolidation, and direction. *Remote Sens. Environ.* **2016**, *185*, 271–283. [[CrossRef](#)]
48. Liberti, M.; Simoniello, T.; Carone, M.T.; Coppola, R.; D'Emilio, M.; Macchiato, M. Mapping badland areas using LANDSAT TM/ETM satellite imagery and morphological data. *Geomorphology* **2009**, *106*, 333–343. [[CrossRef](#)]
49. Chikhaoui, M.; Bonn, F.; Bokoye, A.I.; Merzouk, A. A spectral index for land degradation mapping using ASTER data: Application to a semi-arid Mediterranean catchment. *Int. J. Appl. Earth Obs. Geoinf.* **2005**, *7*, 140–153. [[CrossRef](#)]

50. El Haj El Tahir, M.; Kääb, A.; Xu, C.Y. Identification and mapping of soil erosion areas in the Blue Nile, Eastern Sudan using multispectral ASTER and MODIS satellite data and the SRTM elevation model. *Hydrol. Earth. Syst. Sci.* **2010**, *14*, 1167–1178. [[CrossRef](#)]
51. Vrieling, A.; Rodrigues, S.C.; Bartholomeus, H.; Sterk, G. Automatic identification of erosion gullies with ASTER imagery in the Brazilian Cerrados. *Int. J. Remote Sens.* **2007**, *28*, 2723–2738. [[CrossRef](#)]
52. Yuan, J.; Liu, X.; Li, H.; Wang, R.; Luo, X.; Xing, L.; Wang, C.; Zhao, H. Assessment of Spatial–Temporal Variations of Soil Erosion in Hulunbuir Plateau from 2000 to 2050. *Land* **2023**, *12*, 1214. [[CrossRef](#)]
53. Veraverbeke, S.; Goossens, R.; Vanderstraete, T. Use of ASTER-data for a soil erosion risk model application, Chios Island (Greece). In *Remote Sensing for a Changing Europe*; IOS Press: Amsterdam, The Netherlands, 2009; pp. 117–124. [[CrossRef](#)]
54. Abrams, M. ASTER: Data products for the high spatial resolution imager on NASA's EOS-AM1 platform. *Int. J. Remote Sens.* **2000**, *21*, 847–861. [[CrossRef](#)]
55. Vrieling, A.; de Jong, S.M.; Sterk, G.; Rodrigues, S.C. Timing of erosion and satellite data: A multi-resolution approach to soil erosion risk mapping. *Int. J. Appl. Earth Obs. Geoinf.* **2008**, *10*, 267–281. [[CrossRef](#)]
56. Wohlfart, C.; Winkler, K.; Wendleder, A.; Roth, A. TerraSAR-X and Wetlands: A Review. *Remote Sens.* **2018**, *10*, 916. [[CrossRef](#)]
57. Cruz, H.; Véstias, M.; Monteiro, J.; Neto, H.; Duarte, R.P. A Review of Synthetic-Aperture Radar Image Formation Algorithms and Implementations: A Computational Perspective. *Remote Sens.* **2022**, *14*, 1258. [[CrossRef](#)]
58. Dabboor, M.; Olthof, I.; Mahdianpari, M.; Mohammadimanesh, F.; Shokr, M.; Brisco, B.; Homayouni, S. The Radarsat Constellation Mission Core Applications: First Results. *Remote Sens.* **2022**, *14*, 301. [[CrossRef](#)]
59. Noda, A.; Suzuki, S.; Shimada, M.; Toda, K.; Miyagi, Y. COSMO-SkyMed and ALOS-1/2 X and L Band Multi-Frequency Results in Satellite Disaster Monitoring. In *Proceedings of the 2015 IEEE International Geoscience and Remote Sensing Symposium (IGARSS)*, Milan, Italy, 26–31 July 2015; IEEE: Piscataway, NJ, USA, 2015; pp. 211–214. [[CrossRef](#)]
60. Ling, M.; Chen, J.; Lan, Y.; Chen, Z.; You, H.; Han, X.; Zhou, G. Exploring the Drivers of Soil Conservation Variation in the Source of Yellow River under Diverse Development Scenarios from a Geospatial Perspective. *Sustainability* **2024**, *16*, 777. [[CrossRef](#)]
61. Martínez-Graña, A.; Carrillo, J.; Lombana, L.; Criado, M.; Palacios, C. Mapping the Risk of Water Soil Erosion in Larrodrido (Salamanca, Spain) Using the RUSLE Model and A-DInSAR Technique. *Agronomy* **2021**, *11*, 2120. [[CrossRef](#)]
62. Cook, K.; Agha Karimi, A.; Grinham, A.; McDougall, K. Mapping Erosion Hotspots: Coherent Change Detection in the Quilpie Region, Queensland, Australia. *Remote Sens.* **2024**, *16*, 1263. [[CrossRef](#)]
63. Jiang, C.; Fan, W.; Yu, N.; Nan, Y. A New Method to Predict Gully Head Erosion in the Loess Plateau of China Based on SBAS-InSAR. *Remote Sens.* **2021**, *13*, 421. [[CrossRef](#)]
64. Lu, P.; Zhang, B.; Wang, C.; Liu, M.; Wang, X. Erosion Gully Networks Extraction Based on InSAR Refined Digital Elevation Model and Relative Elevation Algorithm—A Case Study in Huangfuchuan Basin, Northern Loess Plateau, China. *Remote Sens.* **2024**, *16*, 921. [[CrossRef](#)]
65. Sánchez-Crespo, F.A.; Gómez-Villarino, M.T.; Gallego, E.; Fuentes, J.M.; García, A.I.; Ayuga, F. Monitoring of Water and Tillage Soil Erosion in Agricultural Basins, a Comparison of Measurements Acquired by Differential Interferometric Analysis of Sentinel TopSAR Images and a Terrestrial LIDAR System. *Land* **2023**, *12*, 408. [[CrossRef](#)]
66. Shafique, A.; Cao, G.; Khan, Z.; Asad, M.; Aslam, M. Deep Learning-Based Change Detection in Remote Sensing Images: A Review. *Remote Sens.* **2022**, *14*, 871. [[CrossRef](#)]
67. Zhang, Z.; Zhu, L. A Review on Unmanned Aerial Vehicle Remote Sensing: Platforms, Sensors, Data Processing Methods, and Applications. *Drones* **2023**, *7*, 398. [[CrossRef](#)]
68. D'Oleire-Oltmanns, S.; Marzolf, I.; Peter, K.D.; Ries, J.B. Unmanned Aerial Vehicle (UAV) for Monitoring Soil Erosion in Morocco. *Remote Sens.* **2012**, *4*, 3390–3416. [[CrossRef](#)]
69. Mirzaee, S.; Gomez, C.; Pajouhesh, M.; Abdollahi, K. Soil erosion and sediment change detection using UAV technology. In *Remote Sensing of Soil and Land Surface Processes*; Elsevier: Amsterdam, The Netherlands, 2024; pp. 271–279. [[CrossRef](#)]
70. Alexiou, S.; Papanikolaou, I.; Schneiderwind, S.; Kehrlé, V.; Reicherter, K. Monitoring and Quantifying Soil Erosion and Sedimentation Rates in Centimeter Accuracy Using UAV-Photogrammetry, GNSS, and t-LiDAR in a Post-Fire Setting. *Remote Sens.* **2024**, *16*, 802. [[CrossRef](#)]
71. Moore, I.D.; Grayson, R.B.; Ladson, A.R. Digital Terrain Modelling: A Review of Hydrological, Geomorphological, and Biological Applications. *Hydrol. Process.* **1991**, *5*, 3–30. [[CrossRef](#)]
72. Liu, Q.Q.; Chen, L.; Li, J.C. Influences of Slope Gradient on Soil Erosion. *Appl. Math. Mech.* **2001**, *22*, 510–519. [[CrossRef](#)]
73. Buitrago, J.Y.; Martínez, L.J. Digital elevation models (DEM) used to assess soil erosion risks: A case study in Boyaca, Colombia. *Agron. Colomb.* **2016**, *34*, 239–249. [[CrossRef](#)]
74. Mizukoshi, H.; Masamu, A. Use of contour-based DEMs for deriving and mapping topographic attributes. *Photogramm. Eng. Remote Sens.* **2002**, *68*, 83–93.
75. Toutin, T. Elevation modelling from satellite visible and infrared (VIR) data. *Int. J. Remote Sens.* **2001**, *22*, 1097–1125. [[CrossRef](#)]

76. Toutin, T.; Gray, L. State-of-the-art of elevation extraction from satellite SAR data. *ISPRS J. Photogramm. Remote Sens.* **2000**, *55*, 13–33. [[CrossRef](#)]
77. Mondal, A.; Khare, D.; Kundu, S.; Mukherjee, S.; Mukhopadhyay, A.; Mondal, S. Uncertainty of Soil Erosion Modelling Using Open Source High Resolution and Aggregated DEMs. *Geosci. Front.* **2017**, *8*, 425–436. [[CrossRef](#)]
78. Michalopoulou, M.; Depountis, N.; Nikolakopoulos, K.; Boumpoulis, V. The Significance of Digital Elevation Models in the Calculation of LS Factor and Soil Erosion. *Land* **2022**, *11*, 1592. [[CrossRef](#)]
79. Ren, S.; Liang, Y.; Sun, B. Research on sensitivity for soil erosion evaluation from DEM and remote sensing data source of different map scales and image resolutions. *Procedia Environ. Sci.* **2011**, *10*, 1753–1760. [[CrossRef](#)]
80. Datta, P.S.; Schack-Kirchner, H. Erosion Relevant Topographical Parameters Derived from Different DEMs—A Comparative Study from the Indian Lesser Himalayas. *Remote Sens.* **2010**, *2*, 1941–1961. [[CrossRef](#)]
81. Micić Ponjiger, T.; Lukić, T.; Basarin, B.; Jokić, M.; Wilby, R.L.; Pavić, D.; Mesaroš, M.; Valjarević, A.; Milanović, M.M.; Morar, C. Detailed Analysis of Spatial–Temporal Variability of Rainfall Erosivity and Erosivity Density in the Central and Southern Pannonian Basin. *Sustainability* **2021**, *13*, 13355. [[CrossRef](#)]
82. Thomas, J.; Prasannakumar, V.; Vineetha, P. Suitability of space-borne digital elevation models of different scales in topographic analysis: An example from Kerala, India. *Environ. Earth Sci.* **2015**, *73*, 1245–1263. [[CrossRef](#)]
83. Stokstad, E. Hydrology—Scarcity of rain, stream gages threatens forecasts. *Science* **1999**, *285*, 1199–1200. [[CrossRef](#)]
84. De Santos Loureiro, N.; de Azevedo Coutinho, M. A new procedure to estimate the RUSLE EI30 Index, based on monthly rainfall data and applied to the Algarve region, Portugal. *J. Hydrol.* **2001**, *250*, 12–18. [[CrossRef](#)]
85. Stisen, S.; Sandholt, I. Evaluation of remote-sensing-based rainfall products through predictive capability in hydrological runoff modelling. *Hydrol. Process* **2010**, *24*, 879–891. [[CrossRef](#)]
86. Kummerow, C.; Barnes, W.; Kozu, T.; Shiue, J.; Simpson, J. The Tropical Rainfall Measuring Mission (TRMM) sensor package. *J. Atmos. Ocean. Technol.* **1998**, *15*, 809–817. [[CrossRef](#)]
87. Hsu, K.-L.; Gao, X.; Sorooshian, S.; Gupta, H.V. Precipitation estimation from remotely sensed information using artificial neural networks. *J. Appl. Meteorol. Climatol.* **1997**, *36*, 1176–1190. [[CrossRef](#)]
88. Sorooshian, S.; Hsu, K.-L.; Gao, X.; Gupta, H.V.; Imam, B.; Braithwaite, D. Evaluation of PERSIANN system satellite-based estimates of tropical rainfall. *Bull. Am. Meteorol. Soc.* **2000**, *81*, 2035–2046. [[CrossRef](#)]
89. Hou, A.Y.; Kakar, R.K.; Neeck, S.; Azarbarzin, A.A.; Kummerow, C.D.; Kojima, M.; Oki, R.; Nakamura, K.; Iguchi, T. The global precipitation measurement mission. *Bull. Am. Meteorol. Soc.* **2014**, *95*, 701–722. [[CrossRef](#)]
90. Yonaba, R.; Mounirou, L.A.; Keïta, A.; Fowé, T.; Zouré, C.O.; Belemtougri, A.; Kafando, M.B.; Koïta, M.; Karambiri, H.; Yacouba, H. Exploring the Added Value of Sub-Daily Bias Correction of High-Resolution Gridded Rainfall Datasets for Rainfall Erosivity Estimation. *Hydrology* **2024**, *11*, 132. [[CrossRef](#)]
91. Emberson, R.A. Dynamic rainfall erosivity estimates derived from IMERG data. *Hydrol. Earth Syst. Sci.* **2023**, *27*, 3547–3563. [[CrossRef](#)]
92. Wang, W.; Jiang, Y.; Yu, B.; Zhang, X.; Xie, Y.; Yin, B. Evaluation of GPM IMERG-FR Product for Computing Rainfall Erosivity for Mainland China. *Remote Sens.* **2024**, *16*, 1186. [[CrossRef](#)]
93. Serbaji, M.M.; Bouaziz, M.; Weslati, O. Soil Water Erosion Modeling in Tunisia Using RUSLE and GIS Integrated Approaches and Geospatial Data. *Land* **2023**, *12*, 548. [[CrossRef](#)]
94. Li, X.; Ye, X.; Xu, C. Assessment of Satellite-Based Precipitation Products for Estimating and Mapping Rainfall Erosivity in a Subtropical Basin, China. *Remote Sens.* **2022**, *14*, 4292. [[CrossRef](#)]
95. Li, X.; Li, Z.; Lin, Y. Suitability of TRMM Products with Different Temporal Resolution (3-Hourly, Daily, and Monthly) for Rainfall Erosivity Estimation. *Remote Sens.* **2020**, *12*, 3924. [[CrossRef](#)]
96. Teng, H.; Ma, Z.; Chappell, A.; Shi, Z.; Liang, Z.; Yu, W. Improving Rainfall Erosivity Estimates Using Merged TRMM and Gauge Data. *Remote Sens.* **2017**, *9*, 1134. [[CrossRef](#)]
97. Delgado, D.; Sadaoui, M.; Ludwig, W.; Méndez, W. Spatio-temporal assessment of rainfall erosivity in Ecuador based on RUSLE using satellite-based high frequency GPM-IMERG precipitation data. *Catena* **2022**, *219*, 106597. [[CrossRef](#)]
98. Zhu, Q.; Chen, X.W.; Fan, Q.X.; Jin, H.P.; Li, J.R. A new procedure to estimate the rainfall erosivity factor based on Tropical Rainfall Measuring Mission (TRMM) data. *Sci. China Technol. Sci.* **2011**, *54*, 2437–2445. [[CrossRef](#)]
99. Guo, J.; Chen, J.; Qi, S. Impact of Land Use/Cover Change on Soil Erosion and Future Simulations in Hainan Island, China. *Water* **2024**, *16*, 2654. [[CrossRef](#)]
100. Gyssels, G.; Poesen, J.; Bochet, E.; Li, Y. Impact of plant roots on the resistance of soils to erosion by water: A review. *Prog. Phys. Geogr.* **2005**, *29*, 189–217. [[CrossRef](#)]
101. Mamu, A.T.; Wedajo, G.K. Responses of soil erosion and sediment yield to land use/land cover changes: In the case of Fincha’a watershed, upper Blue Nile Basin, Ethiopia. *Environ. Chall.* **2023**, *13*, 100789. [[CrossRef](#)]
102. Zhu, M. Soil erosion risk assessment with CORINE model: Case study in the Danjiangkou Reservoir region, China. *Stoch. Environ. Res. Risk Assess.* **2012**, *26*, 813–822. [[CrossRef](#)]

103. Chen, G.; Zhao, J.; Duan, X.; Tang, B.; Zuo, L.; Wang, X.; Guo, Q. Spatial Quantification of Cropland Soil Erosion Dynamics in the Yunnan Plateau Based on Sampling Survey and Multi-Source LUCC Data. *Remote Sens.* **2024**, *16*, 977. [CrossRef]
104. Fang, H.; Fan, Z. Assessment of Soil Erosion at Multiple Spatial Scales Following Land Use Changes in 1980–2017 in the Black Soil Region, (NE) China. *Int. J. Environ. Res. Public Health* **2020**, *17*, 7378. [CrossRef]
105. Lin, S.; Zou, Y.; He, Y.; Xue, S.; Zhu, L.; Ye, C. A Spatiotemporal Dynamic Evaluation of Soil Erosion at a Monthly Scale and the Identification of Driving Factors in Hainan Island Based on the Chinese Soil Loss Equation Model. *Sustainability* **2025**, *17*, 2361. [CrossRef]
106. Wang, S.; Xu, X.; Huang, L. Spatial and Temporal Variability of Soil Erosion in Northeast China from 2000 to 2020. *Remote Sens.* **2023**, *15*, 225. [CrossRef]
107. Busico, G.; Grilli, E.; Carvalho, S.C.P.; Mastrocicco, M.; Castaldi, S. Assessing Soil Erosion Susceptibility for Past and Future Scenarios in Semiarid Mediterranean Agroecosystems. *Sustainability* **2023**, *15*, 12992. [CrossRef]
108. Panagos, P.; Ballabio, C.; Poesen, J.; Lugato, E.; Scarpa, S.; Montanarella, L.; Borrelli, P. A Soil Erosion Indicator for Supporting Agricultural, Environmental and Climate Policies in the European Union. *Remote Sens.* **2020**, *12*, 1365. [CrossRef]
109. Stefanidis, S.; Mallinis, G.; Alexandridis, V. Multi-Decadal Monitoring of Soil Erosion Rates in South Europe. *Environ. Sci. Proc.* **2023**, *26*, 138. [CrossRef]
110. Sestras, P.; Mircea, S.; Cîmpeanu, S.M.; Teodorescu, R.; Roșca, S.; Bilașco, Ș.; Rusu, T.; Salagean, T.; Dragomir, L.O.; Marković, R.; et al. Soil Erosion Assessment Using the Intensity of Erosion and Outflow Model by Estimating Sediment Yield: Case Study in River Basins with Different Characteristics from Cluj County, Romania. *Appl. Sci.* **2023**, *13*, 9481. [CrossRef]
111. Panagos, P.; Karydas, C.; Borrelli, P.; Ballabio, C.; Meusburger, K. Advances in soil erosion modelling through remote sensing data availability; at European scale. In Proceedings of the Second International Conference on Remote Sensing and Geoinformation of the Environment (RSCy2014), Paphos, Cyprus, 7–10 April 2014. [CrossRef]
112. Chen, J.; Chen, J.; Liao, A.; Cao, X.; Chen, L.; Chen, X.; He, C.; Han, G.; Peng, S.; Lu, M. Global land cover mapping at 30m resolution: A pok-based operational approach. *ISPRS J. Photogramm. Remote Sens.* **2015**, *103*, 7–27. [CrossRef]
113. Friedl, M.A.; McIver, D.K.; Hodges, J.C.F.; Zhang, X.Y.; Muchoney, D.; Strahler, A.H.; Woodcock, C.E.; Gopal, S.; Schneider, A.; Cooper, A.; et al. Global land cover mapping from MODIS: Algorithms and early results. *Remote Sens. Environ.* **2002**, *83*, 287–302. [CrossRef]
114. Bontemps, S.; Defournya, P.; Van Bogaert, E.; Weber, J.L.; Arino, O. GlobCorine—A joint EEA-ESA project for operational land dynamics monitoring at pan-European scale. In Proceedings of the 33rd International Symposium on Remote Sensing of Environment, Stresa, Italy, 4–8 May 2009.
115. Zanaga, D.; Van De Kerchove, R.; Daems, D.; De Keersmaecker, W.; Brockmann, C.; Kirches, G.; Wevers, J.; Cartus, O.; Santoro, M.; Fritz, S.; et al. ESA WorldCover 10 m 2020 v100. Zenodo. Available online: <https://zenodo.org/records/5571936> (accessed on 7 March 2025).
116. Karra, K.; Kontgis, C.; Statman-Weil, Z.; Mazzariello, J.C.; Mathis, M.; Brumby, S.P. *Global Land Use/Land Cover with Sentinel 2 and Deep Learning*; IEEE: Manhattan, NY, USA, 2021; pp. 4704–4707. [CrossRef]
117. Liu, P.; Pei, J.; Guo, H.; Tian, H.; Fang, H.; Wang, L. Evaluating the Accuracy and Spatial Agreement of Five Global Land Cover Datasets in the Ecologically Vulnerable South China Karst. *Remote Sens.* **2022**, *14*, 3090. [CrossRef]
118. Nearing, M.A.; Govers, G.; Norton, L.D. Variability in Soil Erosion Data from Replicated Plots. *Soil Sci. Soc. Am. J.* **1999**, *63*, 1829–1835. [CrossRef]
119. Loughran, R.J. The measurement of soil erosion. *Prog. Phys. Geogr.* **1989**, *13*, 216–233. [CrossRef]
120. Hudson, N.W. Field measurement of soil erosion and runoff. In *FAO Soils Bulletin*; Food & Agriculture Organization: Rome, Italy, 1983; p. 139. Available online: <https://www.fao.org/4/t0848e/t0848e00.htm> (accessed on 27 March 2025).
121. Boix-Fayos, C.; Martínez-Mena, M.; Arnau-Rosalén, E.; Calvo-Cases, A.; Castillo, V.; Albaladejo, J. Measuring soil erosion by field plots: Understanding the sources of variation. *Earth-Sci. Rev.* **2006**, *78*, 267–285. [CrossRef]
122. Stroosnijder, L. Measurement of erosion: Is it possible? *CATENA* **2005**, *64*, 162–173. [CrossRef]
123. Renard, K.G.; Foster, G.R.; Weesies, G.A.; Porter, J.P. RUSLE: Revised universal soil loss equation. *J. Soil Water Conserv.* **1991**, *46*, 30–33. [CrossRef]
124. Mitsova, H.; Hofierka, J.; Zlocha, M.; Iverson, L.R. Modelling topographic potential for erosion and deposition using GIS. *Int. J. Geogr. Inf. Syst.* **1996**, *10*, 629–641. [CrossRef]
125. Phinzi, K.; Ngetar, N.S. The Assessment of Water-Borne Erosion at Catchment Level Using GIS-Based RUSLE and Remote Sensing: A Review. *Int. Soil Water Conserv. Res.* **2019**, *7*, 27–46. [CrossRef]
126. Karaburun, A. Estimation of C factor for soil erosion modeling using NDVI in Buyukcekmece watershed. *Ozean J. Appl. Sci.* **2010**, *3*, 77–85.
127. Ye, S.; Pontius, R.G.; Rakshit, R. A Review of Accuracy Assessment for Object-Based Image Analysis: From Per-Pixel to Per-Polygon Approaches. *ISPRS J. Photogramm. Remote Sens.* **2018**, *141*, 137–147. [CrossRef]

128. Nogueira, K.; Machado, G.L.S.; Gama, P.H.T.; da Silva, C.C.V.; Balaniuk, R.; dos Santos, J.A. Facing Erosion Identification in Railway Lines Using Pixel-Wise Deep-Based Approaches. *Remote Sens.* **2020**, *12*, 739. [[CrossRef](#)]
129. Apostolou, G.; Venieri, K.; Mayoral, A.; Dimaki, S.; Garcia-Molsosa, A.; Georgiadis, M.; Orenge, H.A. Long-Term Settlement Dynamics in Ancient Macedonia: A New Multi-Disciplinary Survey from Grevena (NW Greece). *Land* **2024**, *13*, 1769. [[CrossRef](#)]
130. Papageorgiou, N.; Hadjimitsis, D.G. Evaluation of Soil Loss by Water in Archaeological Landscapes by Using the (R)USLE Model and GIS. The Case Study of Paphos District, Cyprus. In *Digital Heritage. Progress in Cultural Heritage: Documentation, Preservation, and Protection*; Ioannides, M., Fink, E., Cantoni, L., Champion, E., Eds.; EuroMed 2020; Lecture Notes in Computer Science 2020; Springer: Cham, Switzerland, 2021; Volume 12642. [[CrossRef](#)]
131. Agapiou, A.; Lysandrou, V.; Themistocleous, K.; Hadjimitsis, D.G. Risk assessment of cultural heritage sites clusters using satellite imagery and GIS: The case study of Paphos District, Cyprus. *Nat. Hazards* **2016**, *83* (Suppl. S1), 5–20. [[CrossRef](#)]
132. Cuca, B.; Tzouvaras, M.; Agapiou, A.; Lysandrou, V.; Themistocleous, K.; Nisantzi, A.; Hadjimitsis, D.G. Earth observation technologies in service to the cultural landscape of Cyprus: Risk identification and assessment. In Proceedings of the Fourth International Conference on Remote Sensing and Geoinformation of the Environment (RSCy2016), Paphos, Cyprus, 4–8 April 2016; Themistocleous, K., Hadjimitsis, D.G., Michaelides, S., Papadavid, G., Eds.; SPIE: Bellingham, WA, USA, 2016; Volume 9688, p. 96880Y-1. [[CrossRef](#)]
133. Michaelides, K.; Hadjipetrou, S.; Agapiou, A.; Sarris, A.; Klinkenberg, V.; Polidorou, M. Addressing Cultural Heritage Challenges: Applications of Open-Access Remote Sensing Datasets for Monitoring Threats. *Int. Arch. Photogramm. Remote Sens. Spatial Inf. Sci.* **2025**, *XLVIII-M-7-2025*, 67–74. [[CrossRef](#)]
134. Fall, P.L.; Falconer, S.E.; Galletti, C.S.; Shirmang, T.; Ridder, E.; Klinge, J. Long-term agrarian landscapes in the Troodos 1015 foothills, Cyprus. *J. Archaeol. Sci.* **2012**, *39*, 2335–2347. [[CrossRef](#)]
135. Gabriele, M.; Brumana, R.; Previtali, M.; Cazzani, A. A combined GIS and remote sensing approach for monitoring climate change-related land degradation to support landscape preservation and planning tools: The Basilicata case study. *Appl. Geomat.* **2022**, *26*, 497–532. [[CrossRef](#)]
136. Kinsey, M.; Batty, L.; Chapman, H.; Gearey, B.; Ainsworth, S.; Challis, K. Assessing the changing condition of industrial archaeological remains on Alston Moor, UK, using multisensor remote sensing. *J. Archaeol. Sci.* **2014**, *45*, 36–51. [[CrossRef](#)]
137. Lombardo, L.; Tanyas, H.; Nicu, C.I. Spatial modeling of multi-hazard threat to cultural heritage sites. *Eng. Geol.* **2020**, *277*, 105776. [[CrossRef](#)]
138. Agapiou, A.; Lysandrou, V.; Alexakis, D.D.; Themistocleous, K.; Cuca, B.; Argyriou, A.; Sarris, A.; Hadjimitsis, D.G. Cultural heritage management and monitoring using remote sensing data and GIS: The case study of Paphos area, Cyprus. *Comput. Environ. Urban Syst.* **2015**, *54*, 230–239. [[CrossRef](#)]
139. Ciampalini, A.; Frodella, W.; Margottini, C.; Casagli, N. Rapid assessment of geo-hydrological hazards in Antananarivo (Madagascar) historical center for damage prevention. *Geomat. Nat. Hazards Risk* **2019**, *10*, 1102–1124. [[CrossRef](#)]
140. Bagwan, W.A.; Gavali, R.S. Does spatial resolution matter in the estimation of average annual soil loss by using RUSLE? —A study of the Urmodi River Watershed (Maharashtra). India. *Environ. Monit. Assess.* **2024**, *196*, 167. [[CrossRef](#)]
141. Polykretis, C.; Alexakis, D.D.; Grillakis, M.; Agapiou, A.; Cuca, B.; Papadopoulos, N.; Sarris, A. Assessment of water-induced soil erosion as a threat to cultural heritage sites: The case of chania prefecture, crete island, Greece. *Big Earth Data* **2021**, *6*, 561–579. [[CrossRef](#)]
142. Guiney, R.; Santucci, E.; Valman, S.; Booth, A.; Birley, A.; Haynes, I.; Marsh, S.; Mills, J. Integration and Analysis of Multi-Modal 1094 Geospatial Secondary Data to Inform Management of at-Risk Archaeological Sites. *ISPRS Int. J. Geo-Inf.* **2021**, *10*, 575. [[CrossRef](#)]
143. Negula, I.D.; Moise, C.; Lazăr, A.M.; Rîșcuța, N.C.; Cristescu, C.; Dedulescu, A.L.; Mihalache, C.E.; Badea, A. Satellite Remote Sensing for the Analysis of the Micia and Germisara Archaeological Sites. *Remote Sens.* **2020**, *12*, 2003. [[CrossRef](#)]
144. Pagels, J.; Chaouali, M.; Fenwick, C.; Von Rummel, P.; Bebermeier, W. Coupling morphometric analysis and soil erosion modeling for the characterization of the geomorphological setting in the surrounding of the archaeological site of Chimtou (Central Medjerda Valley, Tunisia). *J. Maps* **2024**, *20*, 2332369. [[CrossRef](#)]
145. Brandolini, F.; Compostella, C.; Pelfini, M.; Turner, S. The Evolution of Historic Agroforestry Landscape in the Northern Apennines (Italy) and Its Consequences for Slope Geomorphic Processes. *Land* **2023**, *12*, 1054. [[CrossRef](#)]
146. Brandolini, F.; Kinnaird, T.C.; Srivastava, A.; Turner, S. Modelling the Impact of Historic Landscape Change on Soil Erosion and Degradation. *Sci. Rep.* **2023**, *13*, 4949. [[CrossRef](#)] [[PubMed](#)]
147. Cuca, B.; Agapiou, A. Impact of land-use change and soil erosion on cultural landscapes: The case of cultural paths and sites in Paphos district, Cyprus. *Appl. Geomat.* **2018**, *10*, 515–527. [[CrossRef](#)]
148. Wang, T.; Fu, Z.; Zhang, S.; Li, Z. Water erosion risk assessment and predictive modelling for cultural heritage under climate change: A case study of the Great Wall in the Yellow River Basin, China. *J. Clean. Prod.* **2025**, *510*, 145645. [[CrossRef](#)]
149. Forti, L.; Brandolini, F.; Oselini, V.; Peyronel, L.; Pezzotta, A.; Vacca, A.; Zerboni, A. Geomorphological assessment of the preservation of archaeological tell sites. *Sci. Rep.* **2023**, *13*, 7683. [[CrossRef](#)]

150. Ames, C.J.; Chambers, S.; Shaw, M.; Phillips, N.; Jones, B.G.; Mackay, A. Evaluating erosional impacts on open-air archaeological sites along the Doring River, South Africa: Methods and implications for research prioritization. *Archaeol. Anthropol. Sci.* **2020**, *12*, 103. [[CrossRef](#)]
151. Santos, F.; Calle, N.; Bonilla, S.; Sarmiento, F.; Herrnegger, M. Impacts of soil erosion and climate change on the built heritage of the Pambamarca Fortress Complex in northern Ecuador. *PLoS ONE* **2023**, *18*, e0281869. [[CrossRef](#)] [[PubMed](#)]

Disclaimer/Publisher's Note: The statements, opinions and data contained in all publications are solely those of the individual author(s) and contributor(s) and not of MDPI and/or the editor(s). MDPI and/or the editor(s) disclaim responsibility for any injury to people or property resulting from any ideas, methods, instructions or products referred to in the content.